

# Relating rock mass properties with Lugeon value using multiple regression and nonlinear tools in an underground mine site

İbrahim Ferid Öge<sup>1</sup>  · Mustafa Çırak<sup>1</sup>

Received: 2 February 2017 / Accepted: 16 October 2017 / Published online: 4 November 2017  
© Springer-Verlag GmbH Germany 2017

**Abstract** The Lugeon test is one of the commonly applied field methods for measuring hydraulic conductivity of a rock mass. Understanding hydraulic conductivity is especially necessary when groundwater is present, as it has a direct effect on the construction operations and stability of a structure. Discontinuity orientation, spacing and discontinuous surface quality, and the presence and type of infill play essential roles in permeability of a rock mass. Commonly used rock quality designation (RQD) and discontinuity surface condition rating of the rock mass rating system (Dc) were chosen as predictive parameters. Additionally, depth is involved as a critical predictor and it is observed so. Three variables impacting the Lugeon value are not present in the literature. The importance of each predictor variable was found to be significant while depth contributed more. Simple regression work resulted in insufficient correlation for each single parameter, but indicated they have relevance to the Lugeon value. In addition to linear and nonlinear multiple regression studies, Box-Cox transformation multiple regression was employed and predictions were found to be statistically significant. Among the multiple regression models, a nonlinear model provided the highest prediction performance. Utilization of the adaptive neuro-fuzzy inference system (ANFIS) enabled researchers to predict the Lugeon value precisely, compared to the multiple regression works. Subtractive clustering was employed in order to successfully model the parameters by using ANFIS. The clustering task resulted in a fuzzy inference system structure with three rules. A manually introduced fuzzy inference

system (FIS) structure with 27 rules exhibited low performance when it was compared to the structure generated by subtractive clustering. The findings can be used in the study area since a wide range of rock types, properties and depth were taken into account in the models. Groundwater flow and permeability in jointed rock mass have a complex mechanism with variable fracturing and discontinuity properties within a small area. For prediction work, it is concluded to be beneficial to add the depth parameter to the models for further studies.

**Keywords** Hydraulic conductivity · Lugeon test · Rock mass parameters · Multiple regression · ANFIS

## Introduction

Groundwater has a significant impact on engineered structures built in rock by means of construction operations, rock mass deformation and stability. The degree of the impact depends on its presence and on several engineering parameters as well as moisture sensitivity of the rock material. For underground rock structures, investigation on groundwater pressure and water inflow rate is essential (Aydan et al. 2014; Singh and Singh 2006) since these strongly influence operational issues as well as the stability of the structure and supports. Operational issues may include pump selection and infrastructure design for water discharge, identification of grouting requirements and water sealing. The permeability of surface material also plays an important role for surface structures such as dams and their foundations (Foyo et al. 2005; Karagüzel and Kilic 2000). Discontinuities in a rock mass constitute a dominant path for hydraulic transport (Ren et al. 2015). The terms rock mass hydraulic conductivity, rock mass permeability and secondary permeability are used

✉ İbrahim Ferid Öge  
feridoge@mu.edu.tr

<sup>1</sup> Faculty of Engineering, Department of Mining Engineering, Muğla Sıtkı Koçman University, 48000 Muğla, Kötekli, Turkey

interchangeably in the literature (Fell et al. 2005) and the Lugeon test is one of the constant head-type in situ tests. Alternatively, slug tests can also be applied in highly fractured rock masses (Eryılmaz and Korkmaz 2015; Zlotnik and McGuire 1998). The researchers proposed an identification method for the estimation of hydraulic conductivity.

Since the hydraulic conductivity of rock masses is a complex process, it is drawing researchers' attention. Snow (1969) and Snow (1970) studied hydraulic conductivity of rock masses by taking different discontinuity patterns. Oda et al. (1987) handled randomly and highly jointed rock mass permeability by treating it as a homogeneous anisotropic porous medium. Foyo et al. (2005) proposed the Secondary Permeability Index by utilizing Lugeon tests. The index can be used for classification of a rock mass and treatment necessity. Researchers mentioned the relevance of discontinuity and infill characteristics of the rock mass with hydraulic conductivity. Due to nonuniform distribution of the hydraulic properties of fractures and geometric properties, hydraulic anisotropy develops in a rock mass (Zhang 2013). Nappi et al. (2005) investigated Lugeon values and outcrop discontinuity properties on the outcrops in a region. The anisotropic behavior of hydraulic conductivity was studied and led to complete hydraulic characterization of near-surface rock mass in the research area. The researchers mentioned that depth has an influence on hydraulic conductivity other than the parameters which are taken into account. Leung and Zimmerman (2012) utilized fracture network parameters for estimating two-dimensional hydraulic conductivity for isotropic networks. Zhou et al. (2008) and Rong et al. (2013) studied the interlocking effect of rock blocks and stress-induced reduction of the aperture which has an influence on hydraulic conductivity. Ren et al. (2015) employed numerical analysis in order to assess the hydraulic conductivity anisotropy of a fracture network system. A discrete fracture method for seepage simulation based on a pipe network method is developed to simulate the permeability anisotropy in fracture networks. Pardo et al. (2016) studied excavation-induced damage around an underground opening and its effect on the hydraulic conductivity which leads a relative humidity change in the ventilated opening. Min et al. (2004) carried out numerical modeling in order to assess stress effect on hydraulic conductivity at a fundamental level for fractured rock masses. He et al. (2013) employed numerical analysis techniques which cover elastic deformation in a fractured rock mass. Zhang (2016) carried out laboratory testing on clay rock samples and proposed an empirical model for fracturing-induced permeability by considering the effects of connectivity and conductivity of micro-cracks. Ma et al. (2013) investigated seepage properties of laboratory samples under different confining pressures.

Rigorous approaches which necessitate detailed information on discontinuity properties are being developed for

studying the hydraulic conductivity of jointed rock masses. Collection of various properties of fracture networks is still a practical challenge and is obviously difficult to undertake (Rong et al. 2013). In addition to detailed theoretical studies, employing statistical tools also increases the understanding of field-scale hydraulic conductivity. Kayabasi et al. (2015) employed nonlinear regression and adaptive neuro-fuzzy inference system (ANFIS) modeling in order to relate Lugeon data and discontinuity properties. Data groups from six sites and five different lithologies were utilized in the analysis targeting to estimate the hydraulic conductivity of the rock mass (Lugeon value) empirically. Rock quality designation (RQD) was found to be significantly related to the Lugeon value, while the discontinuity spacing and surface condition rating (Sonmez and Ulusay 1999) represented statistically insignificant behavior, as can be seen from the repeated values. However, the researchers mentioned the importance of those parameters. Assari and Mohammadi (2017) investigated a dam site where heterogeneous hydraulic properties are present in a karstic formation. The researchers conducted a stochastic simulation technique by considering RQD and Lugeon values in order to estimate their spatial character.

### Rock mass, hydraulic conductivity and Lugeon test

Hydraulic conductivity can be measured at both a laboratory scale and a field scale and then can be utilized for calculation of total inflow of groundwater in a particular area. For soil material, all pores or voids are interconnected (Lambe and Whitman 1969) and, in general, gradation, density, porosity, void ratio, saturation degree and stratification affect permeability (Hunt 2005). Generally, intact rock is very well compacted or cemented with mineral grains which contain pores. The pores or voids are not interconnected and they represent at least very low conductivity if the rock mass is not fractured (Fig. 1). Hydraulic conductivity of intact rock and a rock mass are obviously different due to the presence and frequency of discontinuities. Discontinuity condition ( $D_c$ ), namely persistence, tightness, aperture, roughness, infill type and filling thickness, also govern the water flow rate through a rock mass as well as affecting rock mass strength. Field-scale estimation and measurement of hydraulic conductivity becomes more important when the area of interest is a rock mass.

Assuming a laminar flow through smooth joints, hydraulic conductivity,  $K$  (Scesi and Gattinoni 2009):

$$K = \frac{\gamma e^2}{12\eta} = \frac{g e^2}{12\nu} \quad (1)$$

where  $e$  is the joint mean aperture,  $g$  is the gravitational acceleration and  $\nu$ ,  $\gamma$  and  $\eta$  are the kinematic viscosity, the specific

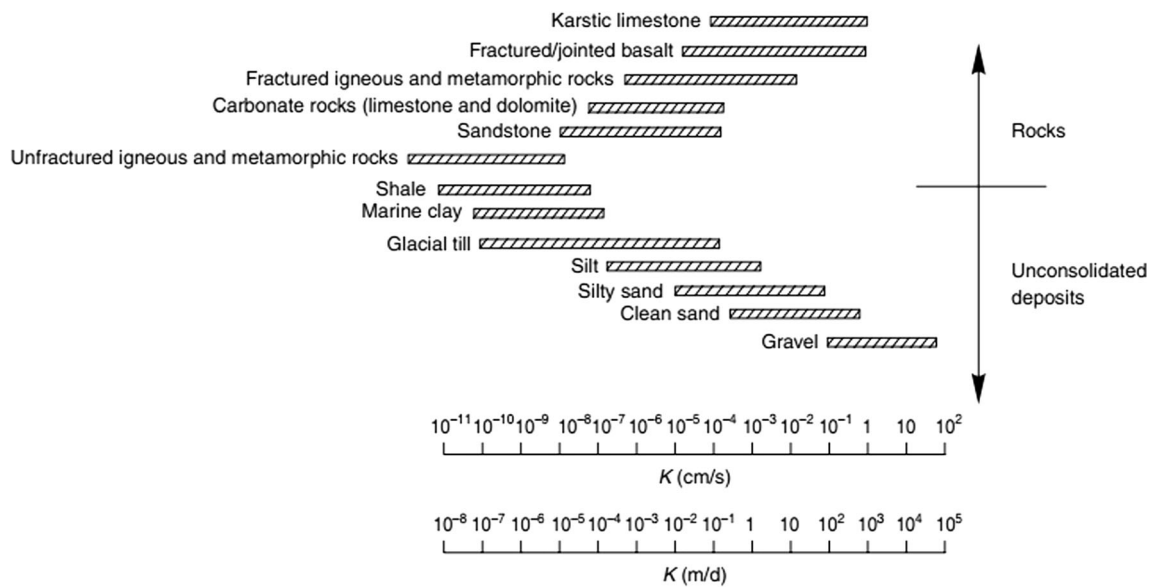


**Fig. 1** Hydraulic conductivity of various geological units (after Atkinson 2000)

weight and the dynamic viscosity of the fluid, respectively.

For laminar flow through smooth-joint groups, Snow (1969, 1970) proposed:

$$K = \frac{e_i^3 f_i g}{12\nu} \tag{2}$$

where  $f_i$  is the frequency ( $m^{-1}$ ) of the  $i^{th}$  discontinuity set.

The Lugeon test is widely employed for in situ estimation of rock mass hydraulic conductivity and sometimes it is called a packer test. This test owes its name to Maurice Lugeon, a geologist who first formulated the method in 1933, (Lugeon 1933). The Lugeon test is a constant head permeability test applied to a particular and isolated interval of a borehole. The testing section is restricted by upper and lower inflatable packers which fit the borehole. A maximum test pressure is identified before the test. The value should be decided bearing in mind that no hydraulic fracturing should occur in the borehole walls. The test is generally conducted at five stages or more. At each stage, a particular percentage of the maximum pressure is kept constant and applied for 10 min. Water loss at each stage

must be recorded. The first-stage pressure must be lower than the maximum pressure. After application of the maximum-pressure stage, lower-pressure stages are supposed to be applied (Quiñones-Rozo 2010; Nappi et al. 2005).

The permeability value obtained in this test gives rough information on the rock discontinuities which intersect the wall of the borehole in the test section (Table 1). Results are expressed in Lugeon (represented by  $Lu$ ) units. A Lugeon is defined as the water loss of 1 l/min per metre length of test section at an effective pressure of 1 MPa (Fell et al. 2005).

$$Lugeon = Lu = (q/L) \times (P_0/P) \tag{3}$$

Here, the Lugeon value is calculated by using water loss  $q$  (lt/min), testing length  $L$ (m), reference pressure  $P_0$  (1 MPa) and pressure applied at a test stage  $P$  (MPa).

The Lugeon test can also be interpreted as suggested by Moye (1955):

$$K = (Q \times C)/(L \times H) \tag{4}$$

Where  $K$  is hydraulic conductivity (m/s),  $Q$  is flow rate ( $m^3/s$ ),  $L$  is the length of the test section (m) and  $r$  is the radius of the

**Table 1** Condition of rock mass discontinuities associated with different Lugeon values (after Quiñones-Rozo 2010)

Lugeon range	Classification	Hydraulic conductivity range (cm/s)	Condition of rock mass discontinuities	Reporting precision (Lugeons)
<1	Very low	$<1 \times 10^{-5}$	Very tight	<1
1–5	Low	$1 \times 10^{-5} - 6 \times 10^{-5}$	Tight	$\pm 0$
5–15	Moderate	$6 \times 10^{-5} - 2 \times 10^{-4}$	Few partly open	$\pm 1$
15–50	Medium	$2 \times 10^{-4} - 6 \times 10^{-4}$	Some open	$\pm 5$
50–100	High	$6 \times 10^{-4} - 1 \times 10^{-3}$	Many open	$\pm 10$
>100	Very high	$> 1 \times 10^{-3}$	Open and closely spaced or voids	>100

hole (m).  $H$  is the net head above the static water table at the centre of the test section (m).  $C$  is given as

$$C = \frac{1 + \ln\left(\frac{L}{2r}\right)}{2\pi} \quad (5)$$

Hoek and Bray (1981) recommend the equation given below which is modified from Moye (1955):

$$ke = \frac{Q \ln\left(\frac{2ML}{D}\right)}{2\pi LH} \quad (6)$$

Here,

$$M = (ke/kp)^{0.5}$$

$kp$  equivalent permeability parallel to the hole  
 $ke$  equivalent permeability normal to the hole  
 $D$  diameter of borehole

Assuming  $ke/kp = 1$  represents homogenous and isotropic conditions,  $M = 1$  and  $1 \text{ Lugeon} = 1.3 \times 10^{-5} \text{ cm/s} = 1.3 \times 10^{-7} \text{ m/s}$  (Fell et al. 2005).

In this study, Lugeon value is taken into account in order to represent rock mass hydraulic conductivity. RQD is used for prediction of Lugeon values since it has a relationship with hydraulic conductivity. The RQD was developed by Deere et al. (1966) to provide a quantitative estimate of rock mass quality from drill core logs. RQD is defined as the percentage of intact pieces longer than 100 mm in total length. RQD, as a commonly used parameter, can also be correlated to fracture density, volumetric joint count or block volume (Palmstrom 2005). In situ stress is represented by depth. Due to the influence of its parameters on hydraulic conductivity, the joint condition rating parameter is involved in the study. The table for Dc rating is given in Table 2.

Here, it is important to mention uncertainty in measuring persistence, especially in boreholes. In the absence of this

data, a zero value is chosen. However, in stratified strata, the persistence rating will be zero, generally.

## Geology of the study area

Lugeon tests and geotechnical borehole logging were conducted in the Soma lignite coal basin. The area is located in the city of Soma in the Manisa Province of Turkey. An open cast mine is under operation in the northern region of the basin where the coal seam lies at shallow depth. In the neighborhood, underground coal mines are in operation at a depth range of 150–400 m (Basarir et al. 2015; Aksoy et al. 2016). The new government and privately owned underground coal mines with depths ranging between 700 and 1200 m are being projected at an approximate distance of 5 km from the mines under operation.

## General geology

Tüysüz and Genç (2013) studied the geology of the study area site. A Pliocene-aged formation named as Deniz is underlain by the Miocene-aged Soma formation. The Deniz Formation contains clastic limnic deposit succession with coal intercalations. The unit was sub-classified in six series by Nebert (1978). They are: sandstone-siltstone-multicolored clay level (P1), upper lignite level (KP1), clay-tuff-marl series (P2ab), clay-sandstone-conglomerate level (P2c), finely grained (siliceous) calcareous level (P3) and tuff-agglomerate (P4 or Plvt) levels. Another rock group situated within the volcanic series, typical outcrops of which are commonly observed in the vicinity of Elmader Village, is flowing breccias. These are formed by thick layers of a lithology with poor but distinctive, variously sized and angular lava gravels as well as lavas in the form of cement pyroclastic flow and rubble units that are composed of latitic, andesitic, rarely dacitic fine lava levels and are interfingering with flowing breccias and lahar levels. The lahar levels contain gravel and blocks with medium-coarse-sized, generally rounded and spherical andesite,

**Table 2** Guidelines for classification of discontinuity conditions (Dc) after Bieniawski 1989

Discontinuity length (persistence)	< 1 m	1 to 3 m	3 to 10 m	10 to 20 m	More than 20 m
Rating	6	4	2	1	0
Separation (aperture)	None	< 0.1 mm	0.1 – 1.0 mm	1–5 mm	More than 5 mm
Rating	6	5	4	1	0
Roughness	Very rough	Rough	Slightly rough	Smooth	Slickensided
Rating	6	5	3	1	0
Infilling (gouge)	None	Hard infilling <5 mm	Hard filling >5 mm	Soft infilling <5 mm	Soft infilling >5 mm
Rating	6	4	2	2	0
Weathering	Unweathered	Slightly weathered	Moderate weathering	Highly weathered	Decomposed
Rating	6	5	3	1	0

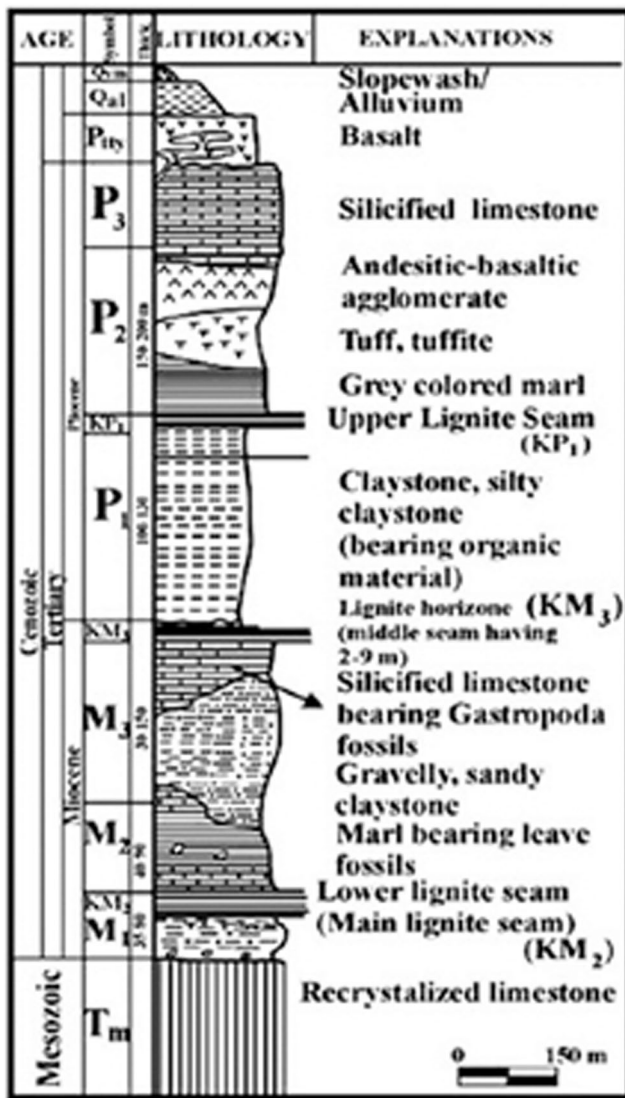


Fig. 2 Generalized stratigraphy of Soma coal basin (after Aksoy et al. 2004)

latite and occasionally dacite compositions. Although they are mostly represented by lava flows, their dykes and vein systems were also observed to cut the deposits and the pyroclastics. Typical examples of them can be witnessed in the southern part of the area, in the east and west of Kocadere and also in the vicinity of the Kızılkaya regions.

The Soma Formation starts with a basement conglomerate unit, discordantly overlaying metamorphic rocks. The conglomerate contains gray-colored, fine-medium-sized grains cemented with sand and silt. A lignite zone with thickness values ranging between 3.5 and 30 m sits over the basement detritus which is symbolized with M1. Called KM2 in the regional Neogene nomenclature, this lignite is of generally hard, massive, black and bright appearance. The lignite quality decreases at the lower sections of KM2 where its clay ratios increase. A bluish-gray-colored marl level overlays the KM2 zone.

Brinkmann and Feist (1970) combine this lithology, defined as M2 with an upper limestone level (M3); they categorized both marl and limestone together as a “marl-calcareous series”. The boundaries between KM2 (lower lignite series) and overlaying marls are very discernible, since the marl directly overlays the M2 lignite zone with a sharp contact. The marls are gray and gray-green-colored, hard and massive. It is a medium-thick layer and contains abundant leaf fossils. In these levels, marls are split into small plates and exhibit almost cardboard shale appearances. The marl series (M2) cut through almost all of each borehole opened in the licensed area, and are widespread and homogenous.

### Structural geology

The study area is located south of Bakırçay Graben which is one of the most important grabens in NW Anatolia. Bakırçay Graben starts with Dikili-Çandarlı at the West, extends to the east, gets narrow eastwardly and changes direction in the vicinity of Soma. The basin is limited at the north by an oblique slip of an active fault which forms a boundary to the Bergama Valley as well. At the south, small fault segments dominated by vertical slip components limit the graben’s boundaries. Dirik et al. (2010a) claimed that the coal basins located at the western part of Soma were developed in the Pliocene-Quaternary period and remained over the Çamlıca Rise which was disintegrated by block faults.

Another structural element in the study area are the folds. The folds are determined by the strike and dips of the deposits, and changing features of the layers through borehole cores are observed. It is known from previous studies that Soma and Deniz Formations are folded. From both Dirik’s (2010) data and the borehole data, some folds are of syn-sedimentary folds (slump structure). The slump nature of the folds is clearly seen through the boreholes, and also from low angled slopes or horizontal features of the layers at much upper and lower sections of the high inclined layer zones. In addition, many medium-scaled folds were also delineated in the area as well. They are symmetrical and of NE-SW-directed folds. Fold structures are especially important for synclinal structures, exploration of underground water and underground water movement. Although the strata dip directions are generally SE, SW and NW directional, the strikes of the layers are NE-SW directionally dominated, but partially NW-SE directed. Layer dips directed NE are rare.

### Data

Four boreholes were subjected to Lugeon testing in the area. These boreholes were drilled in order to conduct geotechnical and hydrogeological investigations for proposed mine access

openings: two shafts and a decline which are being excavated during the study. Borehole depths were adjusted considering the investigated part of the decline and shafts. In the Soma coal basin, a Miocene-aged coal seam (named as KM2) is being mined. Overburden consists of Miocene-aged marl and limestone at the roof of the KM2 coal. Pliocene-aged sedimentary units cover Miocene formations. Volcanic units are also present, especially in Pliocene formations in the form of andesite, basalt or agglomerate. Borehole descriptions and lithology are presented, and in the study, the coal seam is not taken into account (Fig. 2):

BH1: 3 Lugeon tests were conducted along this borehole at depths from 27 to 76 m. Rock types at test locations are agglomeratic, basaltic and andesitic tuff variations. Borehole BH1 is closely located to decline opening.

BH2: 10 Lugeon test results at depths from 8 to 80 m were obtained. Siltstone and conglomerate layers are present with clay and sand. Borehole BH2 is closely located to decline opening.

A geological cross-section around BH-1 and BH-2 is given in Fig. 3.

BH3: 6 Lugeon tests were applied at depths from 40 to 90 m. Fractured andesite was observed from 40 to 140 m, tuffitic agglomerate from 140 to 236 m and andesite from 236 to 306 m. From 306 to 340 m, basalt, andesite and 10-m-thick silicified limestone fractured with slickensides were observed. Borehole BH3 is located at the centerline of mine shaft 1.

BH4: 31 Lugeon tests were applied at depths from 15 to 386 m and from 684 to 772 m. During the first 125 m, the borehole passed through fractured tuff, andesite and agglomerate. From 125 to 228 m, the geological units are siltstone, claystone and marl. From 228 to 276 m, dacite, andesitic agglomerate and tuff reappear. At geological unit contacts, sheared and slickensided discontinuity

surfaces were observed. From 276 to 383 m, Pliocene-aged claystone, conglomerate, siltstone, sandstone and marl layers are present, named as P2C. From 684 to 772 m, P1 Pliocene claystone, siltstone layers, Miocene limestones (M3) and Miocene marl (M2) units are present. Borehole BH4 is located at the centerline of mine shaft 2. A geological cross-section around BH-3 and BH-4 is given in Fig. 4.

For BH-3 and BH-4, in addition to borehole logs, shaft sinking face mapping data is available for the study. It is observed that from 0 to 436 m in BH-3 and 0 to 536 m in BH-4, strike slip faults were observed frequently with small throws (1–2 m). For deeper sections, normal faults start to dominate and strike slip faults disappear. It is thought that fault types may indicate varied mean and deviatoric stresses acting on the rock mass which may lead to a change in the trend of rock mass hydraulic conductivity. Due to the absence of in situ stress data, an exact conclusion cannot be made. However, there are indicators suggesting a considerable variation of in situ stress in the mine field.

In Fig. 5, volcanic and sedimentary rock cores representing a wide range of rock mass quality are given which are taken from different boreholes. A fractured nature is observed while massive zones are present in the field, and different ranges of rock quality were tested by water tests.

Failed tests were identified and finally removed from the study. The common reason is improper insulation of the test interval by the packers. The important point is detecting the leakage and disregarding the test.

### Multiple regression modeling

As given in the study, available literature mentioned the importance of several parameters on rock mass hydraulic

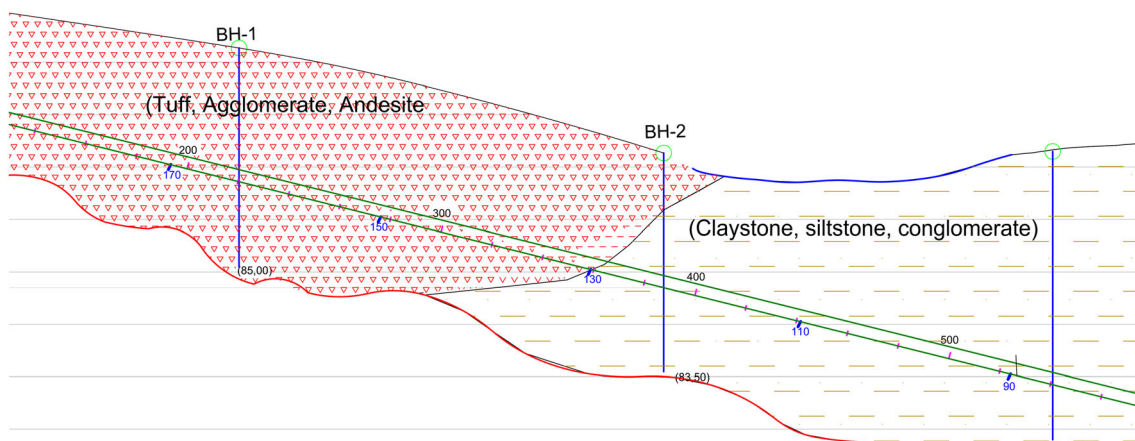


Fig. 3 Geological cross-section around BH-1 and BH-2

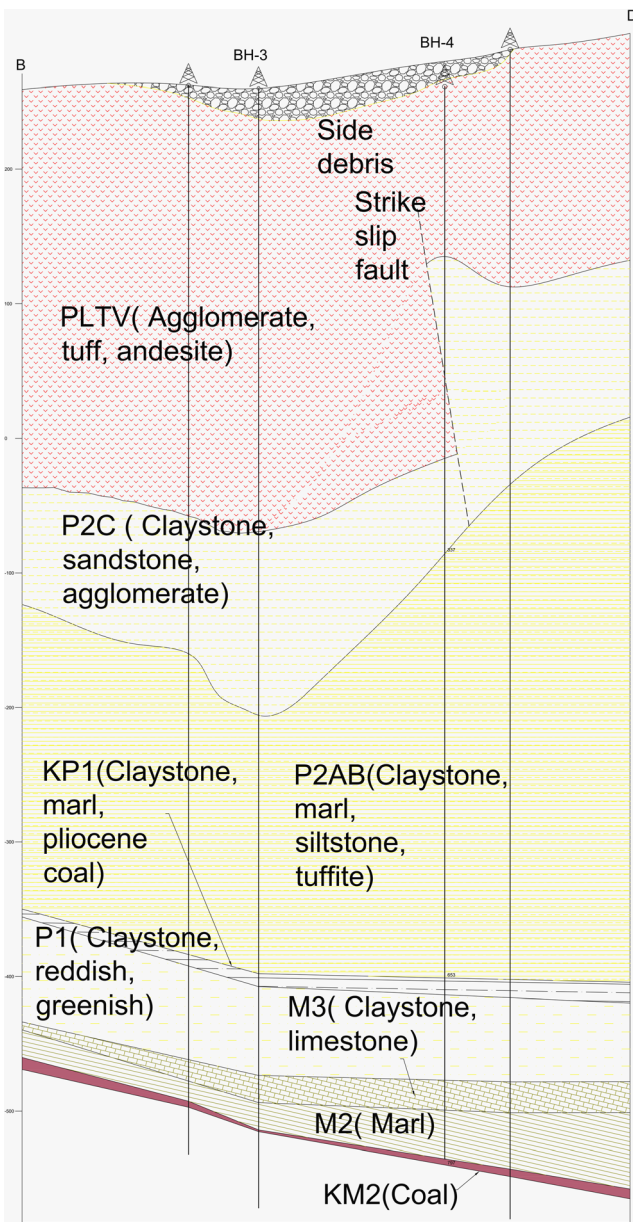


Fig. 4 Geological cross-section around BH-3 and BH-4 (Öge 2017)

conductivity. In situ stress has an influence on rock mass hydraulic conductivity. This influence is reflected by imposing depth in the analyses. Discontinuity density is another important parameter since it identifies the fluid flow path amount in a unit dimension. RQD is chosen to represent discontinuity density in the study. Additionally, discontinuity properties play an important role during fluid flow: persistence and connectivity of the discontinuities, aperture, infilling presence and type, and geometrical character of the discontinuity surfaces. Since a classification system for discontinuity properties is not present in the literature, rock mass rating (RMR) of the Dc is used and it covers most of the parameters under consideration.

Lugeon contours with respect to several combinations are presented in Fig. 6. On top, RQD and depth are used for the

construction of Lugeon contours; in the middle Dc, and depth; at the bottom, Dc and RQD.

Figure 6 reveals the complex relationship among the parameters. Depth is observed to be a strong contributor to Lugeon value. It is also obvious that two variables cannot be satisfactory since a visually observable trend in the contours is not present. However, it is possible to gain an idea about the nature of the parameters. A low Lugeon value is observed for low RQD and poor Dc. Heavily fractured rock mass with clay infills exhibits low hydraulic conductivity. Higher rock mass permeability is observed when  $RQD > 30-40$  and  $Dc > 5$ .

Due to the complex nature of fluid flow through a fractured rock mass, multiple regression modeling is chosen for prediction of Lugeon value. Since the rock mass hydraulic conductivity is represented by Lugeon test measurements which are a function of the above-mentioned parameters, in the study, multiple parameters should be taken into account.

Histograms for the data set are provided in Fig. 7. Depth range is large for the data set and covers a wide range. A sample gap around 500–600 m is observed. The study covers the complete range of RQD. Dc rating varies between 0 and 30. Here, lower-range data is available and represents fair to poor discontinuity surface conditions. For the Lugeon value, a range between 0 and 80 is available. The majority of the values can be classified as very low to moderate hydraulic conductivity, while few data are present for high conductivity.

To comprehend the effect of the independent parameters on the dependent ones, a separate simple linear regression modeling is conducted. The performance of the regression modeling is investigated by the statistical parameters (Table 3). H is the depth in meters.

P values indicate statistical significance for all models.  $R^2$  values are not high and those equations do not offer a sufficiently precise prediction. Statistical indicators show that all variables contribute to the Lugeon value, which led to multiple regression modeling work. The correlation coefficients among the predictive parameters are found to be smaller than 0.11. This means there is not a correlation among them. Kahraman and Kahraman (2016) initially employed simple regression in their study. Later on, they employed multiple regression in order to achieve better predictive performance.

Both linear and nonlinear multiple regression converge to coefficients by minimizing the sum of the squared residuals (SSE). For linear regression, the minimum SSE is derived by solving equations for a given model. If the same data are used, then the same result will be obtained.

In nonlinear regression, a straight-forward solution cannot be proposed, and an iterative algorithm is used in order to estimate unknown coefficients. A nonlinear model compatible with the present data should be selected diligently so that the iterative algorithm systematically adjusts the coefficients to reduce SSE. For each coefficient, an initial value must be





◀ **Fig. 5** (a) Agglomeratic tuff. (b) Silt and sand-banded claystone. (c) Conglomerate with volcanic pebbles and siltstone. (d) Andesite. (e) Agglomeratic andesite. (f) Clay-banded silicified limestone

assigned with which the algorithm starts iterations. During the iteration process, SSE converges to a minimum; thus, it cannot be reduced more and the solution is then obtained. For nonlinear multiple regression, a different model type and initial coefficients alter the prediction. Even for a single model, different initial coefficients may change the results. It can be time-consuming to decide on the model and the initial parameters. In that case, the findings are mostly based on judgment. Omittance of local convergence, rather than the global SSE minimum, is essential during the evaluation of the findings. The same fitting model and initial coefficient were chosen during this study.  $R^2$  values for linear multiple regression are reported but not for nonlinear multiple regression. The

summation of SSE and SSR are not equal to total SS and it totally invalidates  $R^2$  evaluation in nonlinear models (Spiess and Neumeier 2010). In the Box-Cox technique, the model is forced to behave linearly and the  $R^2$  use is acceptable. Linear, nonlinear and Box-Cox multiple regression models and corresponding performance values are given in Table 4. For the multiple regression tasks, the field values are grouped into training and verification groups similar to that done in Basarir et al. (2014) and Yesiloglu-Gultekin et al. (2013). 80% of the data rows are used for training purpose and 20% of the data rows are reserved for verification.

MSE and SSE values are lower for NLMR when it is compared with LMR. Still, the  $R^2$  value for LMR is acceptable. Performance parameters for the Box-Cox technique are presented with respect to the transformed Lugeon value. Using values based on prediction achieves considerably better performance parameters since the Box-Cox technique optimizes

**Fig. 6** Lugeon contour representation for RQD and depth (top), for Dc and depth (middle) and for Dc and RQD (bottom)

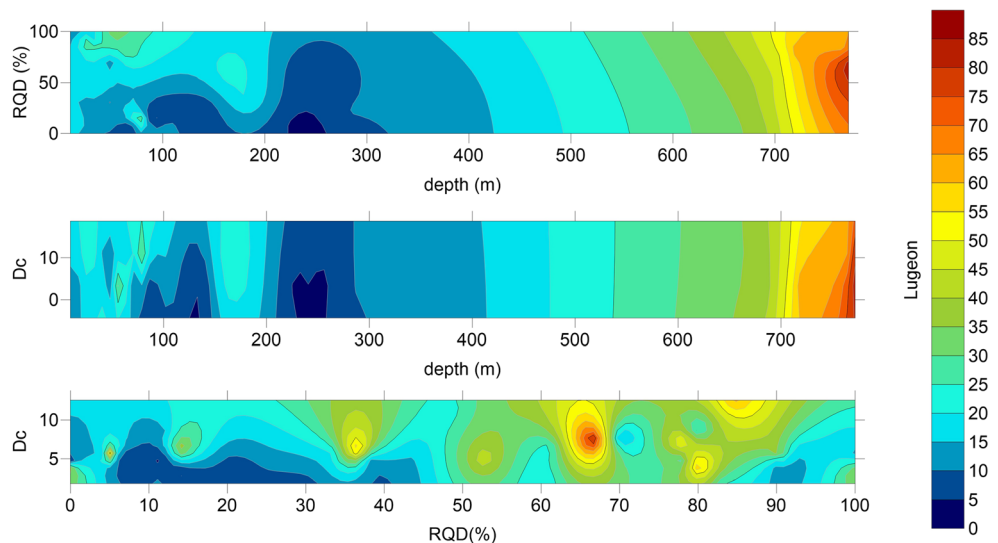


**Fig. 7** Histograms showing the distribution of available field data

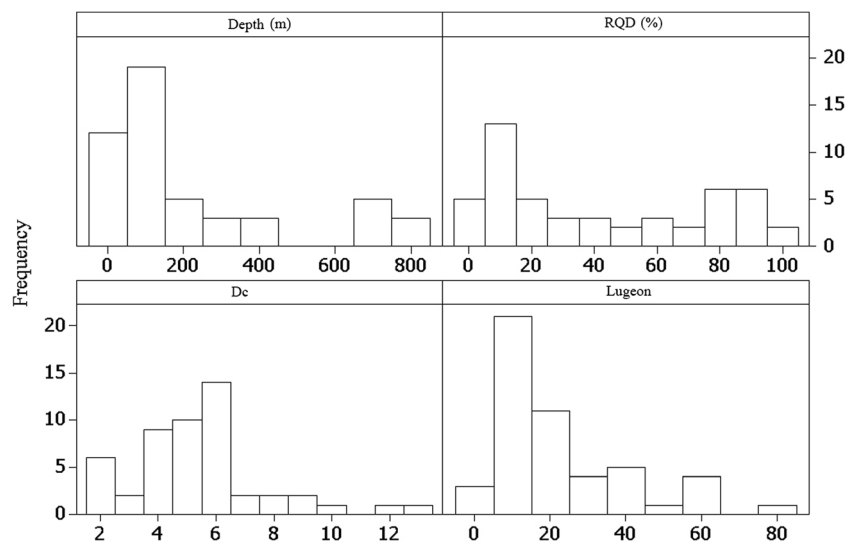


**Table 3** Simple linear regressions

Prediction	R <sup>2</sup>	P value
Lugeon = 10.2 + 0.0565 H	54.6%	P = 0.000
Lugeon = 14.0 + 0.198 RQD	13.0%	P = 0.010
Lugeon = 7.72 + 2.70 Dc	10.4%	P = 0.022

the regression by imposing nonlinear transformation for predicted values and corresponding R<sup>2</sup> values belong to the transformed value. Evaluation of predicted and measured data is presented in the discussion section and the actual performances of the predictions can be investigated rather than statistical parameters. R<sup>2</sup> values for predicted and observed data are also presented and they are above 70%.

### ANFIS

Since three predictive parameters are involved in the study and due to the complex nature of the relationship among the predictive and target variables, ANFIS is employed in the study. ANFIS is capable of handling scattered, complex and nonlinear relationships having multiple variables. Artificial neural networks and fuzzy logic combine the advantage of recognizing the pattern and adapting the method to cope with the changing environment by the incorporation of human knowledge and expertise on the nature of the problem. The FIS is constructed on the foundation of fuzzy set theory, fuzzy if-then rules and fuzzy reasoning (Jang et al. 1997). Khorami et al. (2011) classified the system into three types: Tsukamoto-type FIS (Tsukamoto 1979), Mamdani-type FIS (Mamdani and Assilian 1975) and Takagi–Sugeno type FIS (Sugeno 1985; Sugeno and Kang 1988). ANFIS application can be run on MATLAB (v.9.0.0) and Mamdani and Sugeno types are offered. The Sugeno type has similarities to the Mamdani method in many aspects. The first two parts of the fuzzy inference process are fuzzifying the input and applying the fuzzy operator. However, the main difference between Mamdani and Sugeno is that the Sugeno output membership functions (mf) are either linear or constant. Two fuzzy training types are available: the back-propagation and hybrid types,

which combines back propagation and the least squares method. Jang et al. (1997) explained the inference system is comprised of five layers, each of which involves several nodes, which are described by the node function. Basarir et al. (2014) and Assari and Mohammadi (2017) explained ANFIS architecture and governing equations in detail, incorporated to rock engineering studies.

Initially, a number of mf for each depth, RQD and Dc rating variables were introduced as the three parameters required. Each function was defined in the form of an upper and lower bound and a median. Since each variable has three mf, for each combination, a corresponding rule was defined, which makes 27 rules. Triangular, trapezoidal and Gaussian mf were also imposed for the same logic. This methodology may reflect the nature of the problem; however, it led to an inaccurate prediction of linear relation parameters, possibly due to dividing data sets into small groups. Finally, another FIS is generated by employing subtractive clustering which led to the same number of Gaussian mf. In total, three rules were generated, which increased the number of training samples for each rule. The subtractive clustering method measured the likelihood of each data point and generated clusters by identifying the cluster centre of a potential. This is accomplished based on the density of surrounding data points. The algorithm does the following:

- i. Selects the data point with the highest potential to be the first cluster centre
- ii. Removes all data points in the vicinity of the first cluster centre (as determined by radii), in order to determine the next data cluster and its centre location
- iii. Iterates on this process until all of the data is within the radius of a cluster centre

The subtractive clustering method is an extension of the mountain clustering method proposed by Yager and Filev (1994) and can be applied by MATLAB.

The cluster radius indicates the range of influence of a cluster when you consider the data space as a unit hypercube. Specifying a small cluster radius usually yields many small clusters in the data, and results in many rules. Specifying a large cluster radius usually yields a few large clusters in the

**Table 4** Regression models and performance parameters

Type	Prediction	Training data				Verification data	
		MSE	DFE	SSE	R <sup>2</sup> (%)	R <sup>2</sup> adj. (%)	R <sup>2</sup> pred. (%)
LMR	Lugeon = -6.42 + 0.0507 H + 0.218 RQD + 1.83 Dc	114.7	36	14,749	72%	69.7	74%
NLMR	Lugeon = (H <sup>1.20768</sup> + RQD <sup>1.59227</sup> + Dc <sup>2.33228</sup> ) × 0.0154763	126.787	33	4184	–	–	74%
Box-Cox	Box-Cox(Lugeon) = 0.0374512*H + 0.20944*RQD + 2.05255*Dc Box-Cox (Lugeon) = 1 + (Lugeon <sup>0.569028</sup> - 1) / (0.569 × 16.8576 <sup>-0.431</sup> )	84.23	37	3117	92.41	92.00	71%

data, and results in fewer rules. In the study, rules are identified in the given form and applied with Gaussian mf:

- Rule 1: if depth is  $A_1$  and RQD is  $B_1$  and Dc is  $C_1$  then  $f_1 = p_1 \text{ depth} + q_1 \text{ RQD} + r_1 \text{ Dc} + s_1$
- Rule 2: if depth is  $A_2$  and RQD is  $B_2$  and Dc is  $C_2$ , then  $f_2 = p_2 \text{ depth} + q_2 \text{ RQD} + r_2 \text{ Dc} + s_2$ .
- Rule 3: if depth is  $A_3$  and RQD is  $B_3$  and Dc is  $C_3$ , then  $f_3 = p_3 \text{ depth} + q_3 \text{ RQD} + r_2 \text{ Dc} + s_3$ .

The ANFIS structure constructed for this study is given in Fig. 8.

The structure consists of five layers and three main parameters which are divided into three and Gaussian mf were introduced. As mentioned before, introducing 27 memberships for this combination is possible; however, the structure offering the better result is presented.

### Discussion and performance of predictions

Linear, nonlinear and Box-Cox multiple regression techniques converged to fits, and their performance is close to each other when predicted and estimated Lugeon values are considered. However, nonlinear multiple regression required numerous trials and enhanced understanding of the available data. Although, user-dependent nonlinear regression performance parameters are found to be better when compared to linear regression. However, depending on the trial and error and inspection of each variable, an unsuccessful and nonconvergent solution could be obtained, unlike linear regression. In order to achieve high prediction performance, employing a systematical approach Box-Cox technique is utilized. This approach is less user-dependent and convergence to the same result with a fixed methodology is possible. Box-

Cox transformation applied to Lugeon value improves the performance characteristics of the proposed prediction while altering the linear regression into nonlinear regression. In regression modeling, it is possible to divide available data into training and testing groups. Researchers have preferred a variety of the ratios in their studies; Yilmaz and Yuksek (2009) applied a 1:0.5 ratio for training/test ratio, while Kayabasi et al. (2015) preferred 1:0.2, with the ratio being 1:0.25 in this study.

ANFIS is capable of handling complex behavior and high scatter. The introduction of human expertise to the problem increases the problem-solving capacity of the ANFIS; however, in this study, rather than human preferences, subtractive clustering results in success, in contrast to the study by Kayabasi et al. (2015). The researchers also applied subtractive clustering, but then imposed human expertise and reduced mf numbers in order to improve the performance of prediction.

In order to compare predicted and observed Lugeon values, the overall data set is considered and the error for each data is given. In Basarir et al. (2014), training and testing data were used in regression analyses which enabled comparison of findings by employing the similar approach.

Figure 9 reveals that ANFIS has better prediction performance since the slope of best fit of the data should be close to 1, and a closeness of  $R^2$  to 1 is important. NLMR has the second rank; however, it cannot always be possible to reach this quality since nonlinear behavior must be introduced manually, unlike the Box-Cox technique. LMR has the lowest prediction quality among others. LMR is important when investigating is real relevance exists among the variables and target value or not. When Lugeon error is plotted against the data, again, visually observing the same ranking is possible (Fig. 10).

In addition to  $R^2$  and slope check prediction performance, variation accounted for (VAF) is often used, by comparing the

Fig. 8 ANFIS structure for the study

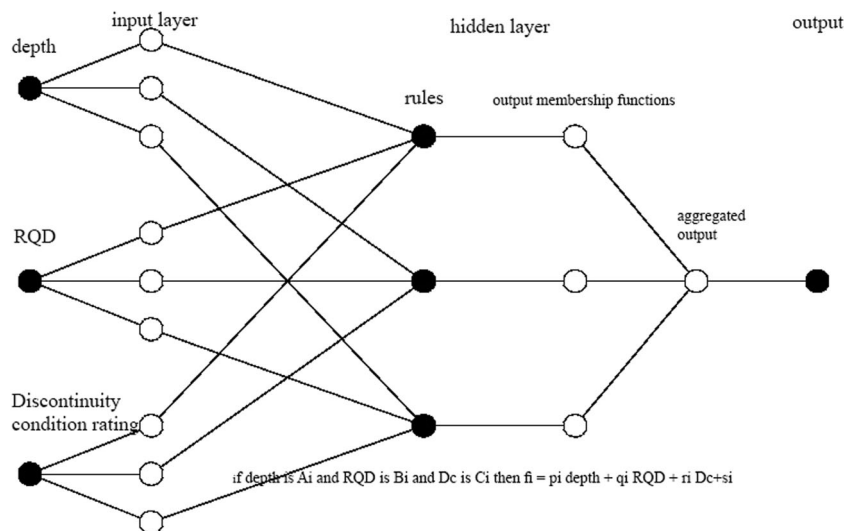
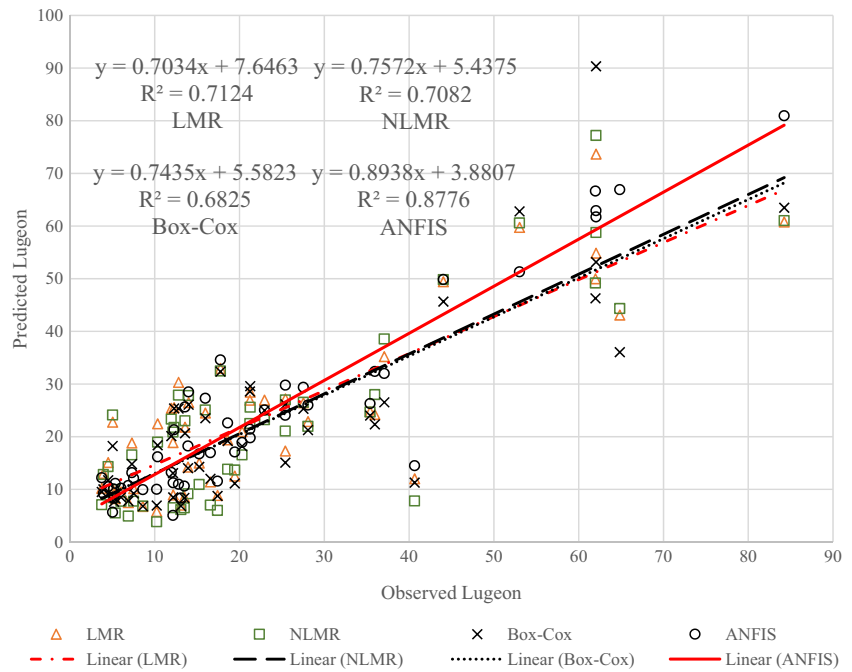


**Fig. 9** Predicted vs. observed Lugeon values



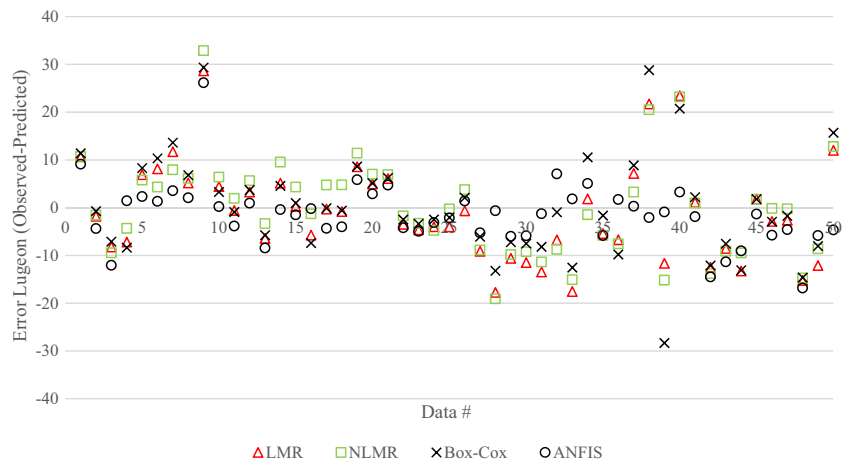
variation of observed values ( $y$ ) with the estimated output of the model ( $y'$ ). High VAF values mean a better model performance. If the observed and predicted values are exactly the same, VAF will be equal to 100%. Root mean square error (RMSE) is another parameter which is commonly used to assess and compare the prediction performances of the tools and models. A lower RMSE value indicates better performance.

$$VAF = \left[ 1 - \frac{\text{var}(y - y')}{\text{var}(y)} \right] \times 100 \quad (7)$$

$$RMSE = \sqrt{\frac{1}{N} \times \sum_{i=1}^N (y - y')^2} \quad (8)$$

Where  $N$  is the sample amount,  $y$  is the observed value and  $y'$  is predicted. The performance parameters are presented in Table 5.

**Fig. 10** Residual error of Lugeon predictions



ANFIS performs better when it is compared to regression modeling; however, the data trend can be easily inspected. Then, the output can be inspected and behavior with respect to the parameters can be discussed.

The influence of depth is clear since the depth varies from around 9 to 800 m. The input for depth is in meters and parameters for depth contribute effectively in the equations.

The significant parameter RQD is found to be positively correlated. In fact, an increased number of discontinuities will lead to higher Lugeon values and vice versa. Barton's (2002)  $Lugeon \approx 1/Q_c$  describes the same trend and it is true if the same  $D_c$  is accepted for the whole range of rock mass structural quality. Here,  $Q_c$  stands for the strength-adjusted  $Q$ -system rating. In the study area, it can be observed that for low RQD, clay or fine material presence increases and it is captured by the correlations, intuitively.

**Table 5** RMSE and VAF indicators for overall and test data

		Linear multiple regression	Nonlinear multiple regression	Box-Cox transformed multiple regression	ANFIS
Training	RMSE	10.16	10.41	10.86	6
	VAF	71.99	70.89	68.37	90.25
	R <sup>2</sup> (pred.)	0.72	0.71	0.69	0.90
Verification	RMSE	9.73	9.07	9.59	9.05
	VAF	72.96	73.63	69.69	90.17
	R <sup>2</sup> (pred.)	0.74	0.74	0.71	0.90
Overall	RMSE	10.08	10.15	10.62	6.72
	VAF	71.23	70.48	67.71	87.73
	R <sup>2</sup> (pred.)	0.71	0.71	0.68	0.88

Lugeon value and discontinuity surface condition have a positive correlation for all analyses, as expected. The rating Dc has a range from 0 to 30. Higher values indicate a better quality of the discontinuity surface. For a lower boundary condition, clay or fine material presence is higher which leads low hydraulic conductivity, while discontinuities having higher values contain less or no infilling. Another important fact is the Dc parameter varies between 0 and 12 in the study area. Thus, higher Dc cases could not be investigated and proposed relationships cannot be applied in rock masses having a Dc greater than 12 due to a possible trend change. The possible trend change can be the smooth and clean nature of the discontinuities with high Dc value.

## Conclusions

This research presents relationships among rock mass classification parameters (Dc and RQD), depth and hydraulic conductivity of the rock mass (Lugeon value). A wide range of rock types and Dc were subjected to Lugeon testing and borehole logging. Finally, successful equations are given in the article. In order to develop more precise relationships, a new rock mass classification system for hydraulic conductivity similar to rock mass classification systems can also be proposed instead of using RQD and Dc values. On the contrary, utilizing pre-existing and commonly used parameters for estimating rock mass permeability will provide higher applicability. Expanding the database used in the study will improve the quality of the relationships. Hydraulic conductivity of the rock masses has great complexity and in-situ testing is crucial. However, in the absence of Lugeon tests, proposed equations can be used in the research area, and involvement of the depth parameter is suggested in further Lugeon value prediction work.

**Acknowledgements** The author thanks Polyak Eyzek Energy Mining A.Ş. and Fina Energy and its personnel for supporting scientific research and providing necessary data for the study. The author presents his gratitude to the geological engineers of Polyak Eyzek, Feridun Emre Yağimli, Ali Türkoğlu and Mehmet Kılıç for providing extensive data on the geology of the area, preparation of geotechnical borehole logs and their additional care during hydraulic testing. Mining engineers Sibel Güventürk and Mustafa Erkayaoğlu, Ph.D. (University of Arizona) are gratefully acknowledged for language editing.

## References

- Aksoy CO, Kose H, Onargan T, Koca Y, Heasley K (2004) Estimation of limit angle using laminated displacement discontinuity analysis in the Soma coal field, western Turkey. *Int J Rock Mech Min Sci* 41(4): 547–556
- Aksoy CO, Küçük K, Uyar GG (2016) Long-term time-dependent consolidation analysis by numerical modelling to determine subsidence effect area induced by longwall top coal caving method, international journal of oil gas and coal. *Technology* 12(1):18–37
- Atkinson LC (2000) The role and mitigation of groundwater in slope stability. *Slope Stab Surf Min* 427–34
- Assari A, Mohammadi Z (2017) Analysis of rock quality designation (RQD) and Lugeon values in a karstic formation using the sequential indicator simulation approach, Karun IV Dam site, Iran. *Bull Eng Geol Environ* 76:771–782. <https://doi.org/10.1007/s10064-016-0898-y>
- Aydan Ö, Ulusay R, Tokashiki N (2014) A new rock mass quality rating system: rock mass quality rating (RMQR) and its application to the estimation of geomechanical characteristics of rock masses. *Rock Mech Rock Eng* 47(4):1255–1276
- Barton N (2002) Some new Q-value correlations to assist in site characterisation and tunnel design. *Int J Rock Mech Min Sci* 39(2):185–216
- Basarir H, Tutluoglu L, Karpuz C (2014) Penetration rate prediction for diamond bit drilling by adaptive neuro-fuzzy inference system and multiple regressions. *Eng Geol* 173:1–9
- Basarir H, Oge IF, Aydin O (2015) Prediction of the stresses around main and tail gates during top coal caving by 3D numerical analysis. *Int J Rock Mech Min Sci* 76:88–97
- Bieniawski ZT (1989) *Engineering rock mass classifications: a complete manual for engineers and geologists in mining, civil, and petroleum engineering*. Wiley
- Brinkmann R, Feist R (1970) Soma dağlarının jeolojisi. *Maden Tetkik ve Arama Dergisi* 74(74)
- Deere DU, Hendron AJ, Patton FD, Cording EJ (1966) Design of surface and near-surface construction in rock. In *The 8th US Symposium on Rock Mechanics (USRMS)*. American Rock Mechanics Association
- Dirik K, Özsayın E, Kahraman B (2010a) Eyzek Sahası'nın (Soma Güneyi) Yapısal Özellikleri. TKİ Genel Müdürlüğü Raporu
- Dirik K., Özsayın E, Kahraman B (2010b) The Report on Structural properties of Eyzek Basin (South of Soma) general directorate of Turkish coal enterprises (in Turkish)
- Eryılmaz GT, Korkmaz S (2015) Kuyu ve Akifer Testlerine Uygulanan Analitik ve Sayısal Yöntemlerle Hidrolik İletkenliğin Belirlenmesi. *Teknik Dergi* 26(126)
- Fell R, MacGregor P, Stapledon D, Bell G (2005) *Geotechnical engineering of dams*. CRC Press, Boca Raton
- Foyo A, Sánchez MA, Tomillo C (2005) A proposal for a secondary permeability index obtained from water pressure tests in dam foundations. *Eng Geol* 77(1):69–82

- He J, Chen SH, Shahrouh I (2013) Numerical estimation and prediction of stress-dependent permeability tensor for fractured rock masses. *Int J Rock Mech Min Sci* 59:70–79
- Hoek E, Bray JD (1981) *Rock slope engineering*. CRC Press
- Hunt RE (2005) *Geotechnical engineering investigation handbook*. CRC Press
- Jang RJS, Sun CT, Mizutani E (1997) *Neuro-fuzzy and soft computing*. Prentice-Hall, Upper Saddle River. (614 pp)
- Kahraman E, Kahraman S (2016) The performance prediction of roadheaders from easy testing methods. *Bull Eng Geol Environ* 75(4):1585–1596. <https://doi.org/10.1007/s10064-015-0801-2>
- Karagüzel R, Kilic R (2000) The effect of the alteration degree of ophiolitic melange on permeability and grouting. *Eng Geol* 57(1):1–2
- Kayabasi A, Yesiloglu-Gultekin N, Gokceoglu C (2015) Use of non-linear prediction tools to assess rock mass permeability using various discontinuity parameters. *Eng Geol* 185:1–9
- Khorami MT, Chelgani SC, Hower JC, Jorjani E (2011) Studies of relationships between free swelling index (FSI) and coal quality by regression and adaptive neuro fuzzy inference system. *Int J Coal Geol* 85(1):65–71
- Lambe TW, Whitman RV (1969) *Soil mechanics*. John Wiley & Sons, Inc., NY
- Leung CT, Zimmerman RW (2012) Estimating the hydraulic conductivity of two-dimensional fracture networks using network geometric properties. *Transp Porous Media* 93(3):777–797
- Lugeon M (1933) *Barrage et Géologie*. Dunod, Paris
- Ma D, Miao XX, Chen ZQ, Mao XB (2013) Experimental investigation of seepage properties of fractured rocks under different confining pressures. *Rock Mech Rock Eng* 46(5):1135–1144
- Mamdani EH, Assilian S (1975) An experiment in linguistic synthesis with a fuzzy logic controller. *Int J Man Mach Stud* 7(1):1–3
- Min KB, Rutqvist J, Tsang CF, Jing L (2004) Stress-dependent permeability of fractured rock masses: a numerical study. *Int J Rock Mech Min Sci* 41(7):1191–1210
- Moye DG (1955) Engineering geology for the snowy mountains scheme. *J Inst Eng Aust* 27(10–11):287–298
- Nappi M, Esposito L, Piscopo V, Rega G (2005) Hydraulic characterisation of some arenaceous rocks of Molise (southern Italy) through outcropping measurements and Lugeon tests. *Eng Geol* 81(1):54–64
- Nebert K (1978) Lignite-bearing Soma Neogene area, western Turkey. *Bulletin of Directorate of Mineral. Res Explor* 90:20–70
- Oda M, Hatsuyama Y, Ohnishi Y (1987) Numerical experiments on permeability tensor and its application to jointed granite at Stripa mine, Sweden. *J Geophys Res Solid Earth* 92(B8):8037–8048
- Öge İF (2017) Prediction of cementitious grout take for a mine shaft permeation by adaptive neuro-fuzzy inference system and multiple regression. *Eng Geol* 228:238–248. <https://doi.org/10.1016/j.enggeo.2017.08.013>
- Palmstrom A (2005) Measurements of and correlations between block size and rock quality designation (RQD). *Tunn Undergr Space Technol* 20(4):362–377
- Pardoen B, Talandier J, Collin F (2016) Permeability evolution and water transfer in the excavation damaged zone of a ventilated gallery. *Int J Rock Mech Min Sci* 85:192–208
- Quiñones-Rozo C (2010) Lugeon test interpretation, revisited. In: *Collaborative management of integrated watersheds*, US Society of Dams, 30th Annual Conference, p 405–414
- Ren F, Ma G, Fu G, Zhang K (2015) Investigation of the permeability anisotropy of 2D fractured rock masses. *Eng Geol* 196:171–182
- Rong G, Peng J, Wang X, Liu G, Hou D (2013) Permeability tensor and representative elementary volume of fractured rock masses. *Hydrogeol J* 21(7):1655–1671. <https://doi.org/10.1007/s10040-013-1040-x>
- Scesi L, Gattinoni P (2009) *Water circulation in rocks*. Springer Science & Business Media
- Singh TD, Singh B (2006) *Elsevier geo-engineering book 5: tunnelling in weak rocks*. Elsevier
- Snow DT (1969) Anisotropic permeability of fractured media. *Water Resour Res* 5(6):1273–1289
- Snow DT (1970) The frequency and apertures of fractures in rock. *Int J Rock Mech Min Sci Geomech Abstr* 7(1):23–40 Pergamon
- Sonmez H, Ulusay R (1999) Modifications to the geological strength index (GSI) and their applicability to stability of slopes. *Int J Rock Mech Min Sci* 36(6):743–760
- Spieß AN, Neumeyer N (2010) An evaluation of R2 as an inadequate measure for nonlinear models in pharmacological and biochemical research: a Monte Carlo approach. *BMC Pharmacol* 10(1):6
- Sugeno M (1985) *Industrial applications of fuzzy control*. Elsevier Science Inc.
- Sugeno M, Kang GT (1988) Structure identification of fuzzy model. *Fuzzy Sets Syst* 28(1):15–33
- Tsukamoto Y (1979) An approach to fuzzy reasoning method. *Advances in fuzzy set theory and applications*
- Tüysüz O, Genç ŞC (2013) *Polyak Eynes (Elmadere) Linyit Sahası Jeolojisi*
- Yager RR, Filev DP (1994) Generation of fuzzy rules by mountain clustering. *J Intell Fuzzy Syst* 2(3):209–219
- Yesiloglu-Gultekin N, Gokceoglu C, Sezer EA (2013) Prediction of uniaxial compressive strength of granitic rocks by various nonlinear tools and comparison of their performances. *Int J Rock Mech Min Sci* 62:113–122
- Yilmaz I, Yuksek G (2009) Prediction of the strength and elasticity modulus of gypsum using multiple regression, ANN, and ANFIS models. *Int J Rock Mech Min Sci* 46(4):803–810
- Zhang L (2013) Aspects of rock permeability. *Front Struct Civ Eng* 7(2):102–116
- Zhang CL (2016) The stress–strain–permeability behaviour of clay rock during damage and recompaction. *J Rock Mech Geotech Eng* 8(1):16–26
- Zhou CB, Sharma RS, Chen YF, Rong G (2008) Flow–stress coupled permeability tensor for fractured rock masses. *Int J Numer Anal Methods Geomech* 32(11):1289–1309
- Zlotnik VA, McGuire VL (1998) Multi-level slug tests in highly permeable formations: 2. Hydraulic conductivity identification, method verification, and field applications. *J Hydrol* 204(1):283–296